

follows, then, that if the arsenic is substitutional, its fluorescence for (111) diffraction should have the same asymmetry as in Fig. 2, but not as pronounced. This was indeed the experimental observation, and is consistent with the conclusion that the arsenic atoms lie on substitutional sites.

The present method is not limited to x-ray diffraction but can be applied to neutron diffraction where a capture process results in the emission of a detectable particle. This would allow light elements to be detected (for example, lithium in silicon) and would extend the range of possible host-solute combinations. The method is limited to reasonably perfect crystal specimens. It may

be possible, however, to use that part of the fluorescence which takes place in a diffraction process to identify the site of the fluorescing species even if the crystal is not perfect.⁴

*Work supported by the Advanced Research Projects Agency through the Materials Science Center of Cornell University.

¹Kindly supplied by Dr. J. R. Patel of the Bell Telephone Laboratories.

²B. W. Batterman, Phys. Rev. **133**, A159 (1964).

³B. W. Batterman and H. Cole, Rev. Mod. Phys. **36**, 681 (1964).

⁴A very interesting discussion of proton channeling in terms of a diffraction process is given by L. D. Chadderton, Thin Films **1**, 157 (1968).

DIELECTRIC CLASSIFICATION OF CRYSTAL STRUCTURES, IONIZATION POTENTIALS, AND BAND STRUCTURES

J. C. Phillips and J. A. Van Vechten*

Bell Telephone Laboratories, Murray Hill, New Jersey 07974

(Received 21 January 1969)

It is shown that dielectrically defined average covalent and ionic energy gaps, E_h and C , respectively, can be used to predict crystal structures and absolute band energies in crystals of formula AB with eight valence electrons per atom pair.

A great many crystals AB containing eight valence electrons per atom pair are known. These range from semiconductors like Si and Ge to ionic crystals like NaCl. Thermochemical data show¹ that the differences in energy for some of these crystals between the "ionic" NaCl structure and the "covalent" zinc-blende structure are as small as 1 kcal/mole. Calculations based on the Born closed-shell model¹ of the cohesive energies of partially ionic crystals are typically in error by 10 kcal/mole, and no accurate method is known for including covalent energies. Thus theoretical predictions of the relative stability of the NaCl and zinc-blende structures have generally been unsuccessful from a quantitative point of view,¹ even when confined to I-VII crystals.

In this note we show that the entire range (IV-IV, III-V, II-VI, and I-VII) of AB crystals can be analyzed dielectrically, using an open-shell energy-band model (random-phase approximation) rather than the Heitler-London picture implicit in the Born model. We begin by defining fractional covalent and ionic characters f_c and f_i of the crystalline cohesion in terms of the average covalent and ionic energy gaps E_h and C defined previously.² Values of E_h and of C have been

tabulated for 68 AB crystals.^{3,4} From these one can calculate f_c and f_i from the definitions

$$f_c = \frac{E_h^2}{E_h^2 + C^2}, \quad f_i = \frac{C^2}{E_h^2 + C^2}. \quad (1)$$

Representative values for f_c are given in Table I for 28 crystals; of course, $f_i = 1 - f_c$. It is seen that the crystals under consideration range from 100% covalent to 96% ionic.

From the table one can see that, as expected, the more ionic crystals have the NaCl structure, while the less ionic ones occur in the zinc-blende or diamond structures. The dividing point between octahedral and tetrahedral coordination is $f_i = 0.785 \pm 0.010$. We have displayed in Fig. 1 the two dimensional population distribution in the $C - E_h$ plane. It is seen that there are three separate regions. In two of these the crystals have (A) the NaCl structure or (D) the diamond or zinc-blende structure. Between these two regions there is a narrow region (B) where wurtzite structures occur.

To understand the microscopic origin of the boundaries between these regions it is convenient to determine the energy of valence-band

Table I. Crystal type and fraction of ionic character for some AB crystals. The ionization potential is quoted for 14 diamond and zinc-blende crystals for which it has been measured and is compared with the value predicted by Eq. (2). The effect of spin-orbit splitting has been removed from the experimental values.

| Crystal | Structure | f_1 | $I_{theory}(eV)$ | $I_{exp}(eV)$ | Crystal | Structure | f_1 |
|---------|-----------|-------|------------------|----------------------|---------|------------|-------|
| Si | diamond | 0.0 | 5.17 | 5.17 ^a | BN | ZB | 0.26 |
| ZnS | ZB and W | 0.62 | 8.09 | 8.73±.3 ^b | BeO | W | 0.62 |
| Ge | diamond | 0.0 | 4.90 | 4.90 ^a | CuBr | W and ZB | 0.74 |
| AlSb | ZB | 0.44 | 5.39 | 5.47 ^c | AgI | ZB and W | 0.77 |
| GaAs | ZB | 0.32 | 5.70 | 5.59 ^d | SiC | ZB and W | 0.18 |
| InP | ZB | 0.44 | 5.74 | 5.72 ^e | ZnO | W | 0.62 |
| ZnSe | ZB and W | 0.63 | 7.43 | 7.55 ^b | CuCl | ZB and W | 0.75 |
| CdS | W and ZB | 0.69 | 7.54 | 7.35 ^b | CdO | NaCl | 0.79 |
| GaSb | ZB | 0.26 | 4.90 | 5.03 ^d | MgSe | NaCl and W | 0.79 |
| InAs | ZB | 0.35 | 5.27 | 5.44 ^d | MgS | NaCl and W | 0.79 |
| ZnTe | ZB and W | 0.61 | 6.31 | 5.89 ^b | MgO | NaCl | 0.84 |
| CdSe | W | 0.70 | 7.08 | 6.88 ^b | LiF | NaCl | 0.92 |
| InSb | ZB | 0.32 | 4.61 | 5.07 ^d | NaCl | NaCl | 0.94 |
| CdTe | ZB | 0.67 | 6.02 | 6.01 ^b | RbF | NaCl | 0.96 |

^aF. G. Allen and G. W. Gobeli, Phys. Rev. **144**, 558 (1966).
^bR. K. Swank, Phys. Rev. **153**, 844 (1967).
^cT. E. Fischer, Phys. Rev. **139**, A1228 (1965).
^dM. L. Cohen and J. C. Phillips, Phys. Rev. **139**, A912 (1965).
^eT. E. Fischer, Phys. Rev. **142**, 519 (1966).

states absolutely relative to vacuum. This has been done for the highest valence state for several diamond- and zinc-blende-type crystals by measurements of ionization energies I_{AB} of single crystals cleaved in vacuum. We have fitted the experimental values shown in Table I with the

expression

$$I_{AB}^2 = I_0^2(d) + C_{AB}^2. \tag{2}$$

Here I_0 is the ionization potential of a purely covalent diamond-type crystal with nearest-neighbor spacing d ; it is assumed that $I_0 = Jd^n$, where J and n are constant. The ionic energy gap C_{AB} has the values determined previously.^{2,3}

Because ionization potentials have been measured on only 14 vacuum-cleaved crystals of diamond and zinc-blende types, (2) must be regarded as tentative and subject to further refinement. It does fit all the current experimental values quite well (Table I).

For some time the valence difference ΔZ has been used to fit both direct and indirect interband transitions in horizontal sequences of AB crystals,⁵ e.g., Ge, GaAs, ZnSe, CuBr. The electronegativity parameter C can be regarded as the generalization of this ΔZ parameter to vertical and skew sequences. Using equations analogous to (2), we have successfully predicted the interband transition energies of 19 diamond, zinc-blende, and wurtzite crystals without recourse to solution of the wave equation or even Fourier

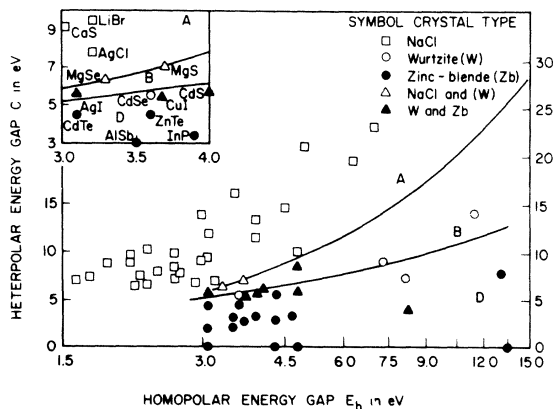


FIG. 1. Crystal type distribution in E_h - C plane. The boundary shown between regions B and D is where we calculate the top of the valence band at Γ is degenerate with that at X . The boundary shown between A and B is where $f_i = 0.785$.

analysis of the crystal potential. The rms error associated with our prediction of 67 energy differences in 19 crystals is 0.23 eV, compared with 0.49 eV for 65 energy differences in 17 crystals in pseudopotential calculations.⁶ For purposes of illustration, several energy differences for four crystals are shown in Table II; note particularly the indirect gaps in GaSb.⁷ We have also predicted band structures for several crystals for which experimental values are not available, e.g., GaN.

Combining our results on ionization potentials with those on both direct and indirect interband transitions, we find the following: (i) The valence "bandwidth" $W \equiv \Gamma_{15}^v - X_5$ decreases as C increases, eventually becoming negative. (ii) The position of the highest valence level at X (X_4 in diamond, X_5 in zinc-blende crystals) is approximately independent of C and depends only on d . (iii) The boundary between tetrahedral and octahedral coordination is well-defined only in the region shown by the inset in Fig. 1. There the boundary occurs when $X_5 - \Gamma_{15}^v = 1.5(d_{Si}/d)^2$. (iv) The boundary between domains B and D occurs when $W = 0$.

The last statement concerning the difference between wurtzite and zinc-blende structures requires qualification. Looking down the c axis of a wurtzite crystal one sees that the trigonal con-

figuration of three atoms bound to B eclipses that bound to A , whereas in the zinc-blende structure the two configurations are staggered. The situation is similar to the rotational barrier in ethane and related molecules. In a homopolar system the staggered conformation is favored, because of the increased kinetic energy in the eclipsed conformation, which generates negative long-range bond orders.⁸ In a sufficiently heteropolar crystal the situation is reversed, as one can show from pseudopotential calculations.⁹ In discussing subtle differences of this kind more precise criteria can be obtained by Fourier analysis of the crystal potential.⁹

In summary, we have found that many of the electronic and structural properties of this large family of crystals can be described by a simplified band model. The closed-shell or Heitler-London effects (which manifest themselves in optical spectra as strong exciton lines) are found to be quantitatively unimportant for discussing phase transitions from tetrahedral to octahedral coordination. (Together with size effects¹ exciton interactions probably stabilize the CsI structure, however.) The present analysis also includes some effects of d -core states and low-lying, alkaline-earth, conduction-band d resonances,³ and it is believed that a similar dielectric approach would prove fruitful for transition-

Table II. Interband energy differences in four zinc-blende crystals. The three values quoted are experiment, our dielectric values, and the pseudopotential value of Ref. 6. The effect of spin-orbit splitting has been removed from the experimental values.

| Crystal | $\Gamma_1^c - \Gamma_{15}^v$ | $X_1^c - \Gamma_{15}^v$ | $L_1^c - \Gamma_{15}^v$ | $X_1^c - X_5^v$ | $\Lambda_1^c - \Lambda_3^v$ | $\Gamma_{15}^c - \Gamma_{15}^v$ | $L_3^c - L_3^v$ |
|---------|------------------------------|-------------------------|-------------------------|-------------------|-----------------------------|---------------------------------|-------------------|
| GaAs | 1.55 ^a | 1.9 ^b | - | 4.99 ^a | 3.04 ^a | 4.2 ^c | 6.4 ^b |
| | 1.55 | 2.37 | 1.89 | 4.81 | 3.11 | 4.28 | 6.23 |
| | 1.4 | 1.8 | 1.7 | 4.0 | 2.6 | 4.5 | 6.0 |
| GaSb | 1.0 ^b | 1.4 ^d | 1.1 ^b | 4.20 ^a | 2.26 ^a | 3.37 ^a | 5.5 ^a |
| | 1.00 | 1.36 | 1.17 | 3.84 | 2.41 | 3.43 | 5.27 |
| | 0.8 | 2.1 | 1.6 | 3.8 | 2.3 | 4.4 | 5.6 |
| InAs | 0.5 ^b | - | - | 4.70 ^a | 2.64 ^a | 3.7 ^c | 6.1 ^b |
| | 0.56 | 2.14 | 1.45 | 4.25 | 2.51 | 3.90 | 5.65 |
| | 0.5 | 2.1 | 1.6 | 3.9 | 2.3 | 4.6 | 5.7 |
| InSb | 0.5 ^b | - | - | 4.08 ^a | 2.13 ^a | 3.27 ^a | 5.25 ^a |
| | 0.39 | 1.40 | 1.01 | 3.48 | 2.05 | 3.21 | 4.87 |
| | 0.6 | 2.0 | 1.5 | 3.5 | 2.1 | 4.1 | 5.1 |

^aM. Cardona, K. L. Shaklee, and F. H. Pollak, Phys. Rev. **154**, 696 (1967).

^bRef. 6.

^cM. L. Cohen and J. C. Phillips, Phys. Rev. **139**, A912 (1965), and unpublished results.

^dRef. 7.

metal salts as well as for more complicated, tetrahedrally coordinated semiconductors.¹⁰

* Fannie and John Hertz Foundation Fellow.

¹M. P. Tosi, *Solid State Phys.* **16**, 68 (1965).

²J. C. Phillips, *Phys. Rev. Letters* **20**, 550 (1968).

³J. A. Van Vechten, to be published.

⁴When a given crystal occurs in more than one structure, the structure listed first in Table I is the one whose dielectric constant is used to determine C .

⁵F. Herman, *J. Electron.* **1**, 103 (1955); M. Cardona and D. L. Greenaway, *Phys. Rev.* **131**, 98 (1963).

⁶M. L. Cohen and T. K. Bergstresser, *Phys. Rev.* **141**, 789 (1966).

⁷B. B. Kosicki, A. Jayaraman, and W. Paul, *Phys. Rev.* **172**, 764 (1968).

⁸J. A. Pople and G. A. Segal, *J. Chem. Phys.* **43**, S136 (1965).

⁹T. K. Bergstresser and M. L. Cohen, *Phys. Rev.* **164**, 1069 (1967), and unpublished results.

¹⁰A. S. Borshchevskii *et al.*, *Phys. Status Solidi* **21**, 9 (1967).

COHERENT AND INCOHERENT RADIATION FROM OPTICALLY EXCITED SURFACE PLASMONS ON A METAL GRATING*

David Beaglehole

Physics Department, University of Maryland, College Park, Maryland 20742
(Received 26 December 1968)

Excitation of surface charge waves (surface plasmons) produces intensity anomalies in the light reflected from a metal grating. We demonstrate that coupling occurs for both s - and p -polarized light if the grating lines are oblique to the plane of incidence, provided there is a component of the incident electric field along the direction of surface-wave propagation. We have measured the magnitude, phase, and direction of the plasmon electric field, and find Fano's theory confirmed. Underlying the coherent radiation we observe a small incoherent component resulting from spontaneous emission by the surface plasmons.

That electromagnetic waves can run along a metal surface whose dielectric constant ϵ is less than -1 is well known. Many years ago Wood¹ observed anomalies in the intensity of p -polarized light diffracted from a metal grating. Fano² explained the anomalies as being due to the resonant excitation of surface waves. He pointed out that this occurs when the incident light, phase modulated by the periodic grating structure, contains a component whose wavelength just matches that of the surface waves. To satisfy the boundary conditions at the surface it is then necessary for there to be an additional reflected field, which interferes with the background reflected field and produces the observed anomalies. p polarization is required to give an incident electric field varying in the direction of surface-wave propagation.

Phase modulation of the incident beam builds up coherent fields at the surface whose momenta along the surface are given by the relation $\vec{k}_s' = \vec{k}_s + n\vec{K}$, where if λ is the incident wavelength, θ the angle of incidence, and d the grating spacing, then $k_s = 2\pi \sin\theta/\lambda$ and $K = 2\pi/d$, and n is an integer. Surface waves are excited whenever $\vec{k}_s' = \vec{k}_p$, the surface-wave momentum. Since surface waves have a momentum only a little great-

er than $2\pi/\lambda$, $k_p^2 - (2\pi/\lambda)^2 = 1/(|\epsilon| - 1)$, the anomalies occur, as Fano explained, where a higher order diffracted beam has just disappeared into the surface.

In the last few years there has been a renewed interest in the properties of surface-charge waves (or surface plasmons). Teng and Stern³ excited these waves on a grating by the electric fields associated with a beam of electrons, and observed spontaneous emission of light. They pointed out that waves running perpendicular to the grating lines would not propagate when their wavelength just matched the grating spacing, and indeed this property had already been observed of the grating anomalies by Stewart and Galloway.⁴ Recently more data on several metals have been presented by Ritchie *et al.*⁵ Teng and Stern and Ritchie *et al.* have shown that the plasmons follow roughly the dispersion relation above.

It is surprising, however, that the resonant electric fields have not before been explicitly measured. In this Letter we demonstrate that when the waves run at an angle to the plane of incidence, they may be stimulated by either s - or p -polarized light. We separate the fields associated with the charge waves from those of the background, and measure the magnitude, direc-